the plant journal

SEB Society for Experimental Biology

The Plant Journal (2012) **71**, 712–723 doi: 10.1111/j.1365-313X.2012.05013.x

The cyclophilin ROC1 links phytochrome and cryptochrome to brassinosteroid sensitivity

Santiago A. Trupkin[1], Santiago Mora-García[2] and Jorge J. Casal[1,2,*]

[1]*IFEVA, Facultad de Agronomía, Universidad de Buenos Aires and CONICET, 1417-Buenos Aires, Argentina, and*

[2]*Fundación Instituto Leloir, Instituto de Investigaciones Bioquímicas de Buenos Aires–CONICET, C1405BWE Buenos Aires, Argentina*

Received 31 August 2011; revised 21 March 2012; accepted 22 March 2012; Published online 06 July 2012.

*For correspondence (e-mail casal@ifeva.edu.ar).

SUMMARY

Although multiple photoreceptors converge to control common aspects of seedling de-etiolation, we are relatively ignorant of the genes acting at or downstream of their signalling convergence. To address this issue we screened for mutants under a mixture of blue plus far-red light and identified *roc1-1D*. The *roc1-1D* mutant, showing elevated expression of the *ROTAMASE CYCLOPHILIN 1* (*ROC1/AtCYP18-3*) gene, and partial loss-of function *roc1* alleles, has defects in phytochrome A (phyA)-, cryptochrome 1 (cry1)- and phytochrome B (phyB)-mediated de-etiolation, including long hypocotyls under blue or far-red light. These mutants show elevated sensitivity to brassinosteroids in the light but not in the dark. Mutations at brassinosteroid signalling genes and the application of a brassinosteroid synthesis inhibitor eliminated the *roc1* and *roc1-D* phenotypes. The *roc1* and *roc1-D* mutants show altered patterns of phosphorylation of the transcription factor BES1, a known point of control of sensitivity to brassinosteroids, which correlate with the expression levels of genes directly targeted by BES1. We propose a model where perception of light by phyA, cry1 or phyB activates ROC1 (at least in part by enhancing its expression). This in turn reduces the intensity of brassinosteroid signalling and fine-tunes seedling de-etiolation.

Keywords: ***ROTAMASE CYCLOPHILIN 1*, phytochrome, cryptochrome, brassinosteroid, Arabidopsis.**

INTRODUCTION

Light triggers profound changes in seedling growth and development upon emergence of the shoot from the soil. In *Arabidopsis thaliana*, light inhibits the growth of the hypocotyl and promotes the expansion of the cotyledons, the organisation of the photosynthetic apparatus and the synthesis of photo-protective pigments (Chen *et al.*, 2004; Jiao *et al.*, 2007). Exposure of the seedling to light activates phytochromes (Quail, 2005) and cryptochromes (Cashmore *et al.*, 1999) among other photoreceptors. In the dark, phytochromes are synthesised in the inactive red-light absorbing Pr form, which upon light absorption is transformed to the active far-red light absorbing Pfr form. There are five phytochrome genes (*PHYA* to *PHYE*) in Arabidopsis. phyA and phyB are quantitatively the most important phytochromes during seedling de-etiolation under far-red light or red light, respectively (Quail, 2005). Cryptochromes are UV-A/blue light photoreceptors, and there are two cryptochrome genes (*CRY1* and *CRY2*) in Arabidopsis. The main blue-light receptor during de-etiolation is cry1 (Cashmore *et al.*, 1999). The action of phytochromes and cryptochromes converges not only to produce largely similar morphological and physiological de-etiolation responses but also to cause similar long-term changes in the transcriptome after the dark to light transition (Ma *et al.*, 2001; Wang *et al.*, 2002a; Tepperman *et al.*, 2004; Jiao *et al.*, 2005). Under the input of strong natural light signals, the action of phytochromes and cryptochromes tends to be redundant (Sellaro *et al.*, 2010).

Comparatively little attention has been paid to the identification of components acting downstream of both phytochrome and cryptochrome. The best characterised pathway involves the E3 ligase CONSTITUTIVE PHOTOMORPHOGENESIS 1 (COP1) and its target ELONGATED HYPOCOTYL 5 (HY5), a bZIP transcription factor (Yi and Deng, 2005). *HY5*, *HOMOLOG OF HY5* (*HYH*), *SUPPRESSOR OF PHYA 1* (*SPA1*) and *SPA4* are central to the synergistic convergence of phyB

and cry1 signalling that creates a hysteretic switch (Sellaro *et al.*, 2009). Genes required for both phyA and cry signalling pathways include the mutually interacting bHLH protein genes *LONG HYPOCOTYL IN FAR-RED* (*HFR1*) (Duek and Fankhauser, 2003) and *KIDARI* (*KDR*) (Hyun and Lee, 2006), the bHLH transcription factor *MYC2* (Yadav *et al.*, 2005), the bZIP transcription factor *G-BOX-BINDING FACTOR 1* (*GBF1*) (Mallappa *et al.*, 2006), the cytoplasmic Ca^{2+}-binding protein *SUB1* (Guo *et al.*, 2001) and SPA1 (Hoecker *et al.*, 1999; Lian *et al.*, 2011; Liu *et al.*, 2011).

The aim of this work is to identify additional signalling components affecting (at least) both phyA- and cry-mediated de-etiolation. We designed a mutant screening protocol based on de-etiolation under a blue plus far-red light mixture. The molecular, genetic and physiological characterisation of the selected mutant points to the cyclophilin gene *ROTAMASE CYCLOPHILIN 1* (*ROC1/AtCYP18-3*) as a link between phytochrome/cryptochrome signalling and brassinosteroid sensitivity.

RESULTS

The 84461-2 mutant shows impaired de-etiolation under blue and far-red light

To identify new signalling components involved in both phyA and cry pathways, we screened a collection of transgenic Arabidopsis 35S-cDNA lines (LeClere and Bartel, 2001) for mutants showing impaired de-etiolation under a mixture of blue and far-red light. The combination of 2 μmol m^{-2} per sec of blue light plus 1 μmol m^{-2} per sec of far-red light was chosen because in preliminary tests it yielded short hypocotyls in the wild type (WT), weak defects in the *phyA* or *cry1* mutants and long hypocotyls in the *phyA cry1* double mutant. The 84461-2 mutant was isolated in this screening.

The 84461-2 mutant showed WT morphology in the dark (Figure 1a). Inhibition of hypocotyl elongation and cotyledon unfolding are induced by far-red light perceived by phyA, by blue light perceived by phyA, cry1 and cry2, and by red light perceived by phyA and phyB (Ahmad and Cashmore, 1993; Nagatani *et al.*, 1993; Parks and Quail, 1993; Reed *et al.*, 1993; Lin *et al.*, 1998; Neff and Chory, 1998). Compared with the WT, the 84461-2 mutant showed long hypocotyls and poorly unfolded cotyledons under blue and under far-red light and normal hypocotyls and more unfolded cotyledons under red light (Figure 1a–c). Anthocyanin accumulation is induced by far-red light perceived by phyA and by blue light perceived by phyA, cry1 and cry2 (Neff and Chory, 1998; Poppe *et al.*, 1998; Mockler *et al.*, 1999). The 84461-2 mutant showed reduced anthocyanin accumulation under blue or far-red light (Figure 1d). Chlorophyll synthesis is reduced when the seedlings are exposed for several days to far-red light perceived by phyA before being transferred to white light (Barnes *et al.*, 1996). The 84461-2 mutant showed reduced blocking of greening by far-red light (Figure 1e).

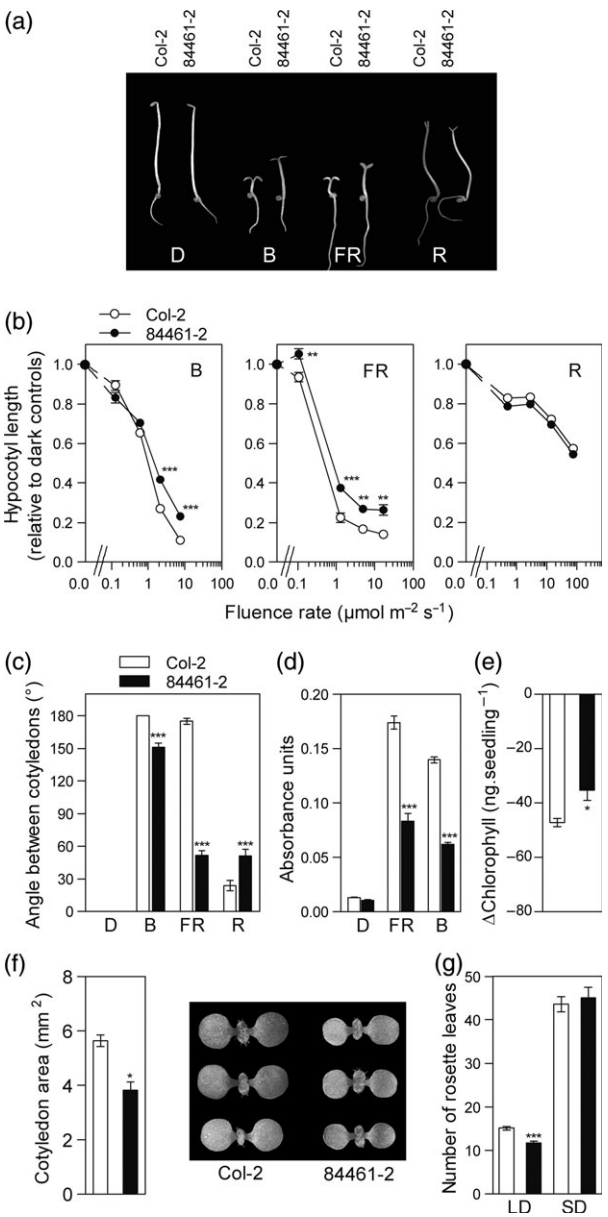

Figure 1. Impaired photomorphogenic responses in the 84461-2 mutant.
(a) Representative seedlings grown under continuous blue light (B, 2 μmol m^{-2} per sec), far-red light (FR, 3 μmol m^{-2} per sec), red light (R, 5 μmol m^{-2} per sec) or darkness (D). (b) Fluence-rate response of hypocotyl length under continuous blue, far-red or red light.
(c) Cotyledon unfolding under conditions described in (a). (d) Anthocyanin levels under continuous far-red light (18 μmol m^{-2} per sec), blue light (15 μmol m^{-2} per sec) or darkness. (e) Blocking of greening by continuous far-red light (3 days, 7 μmol m^{-2} per sec) compared with darkness before transfer to fluorescent white light (1 day, 30 μmol m^{-2} per sec) (difference in chlorophyll content between darkness and far-red light). (f) Cotyledon area in seedlings grown under long days (16 h of fluorescent white light, 8 h of darkness). (g) Flowering time (number of rosette leaves at bolting) under short days (SD, 8 h of fluorescent white light, 16 h of darkness) or long days (LD, 16 h of fluorescent white light, 8 h of darkness).
Seedlings were 3 (a–e) or 11 (f) days old. Each datum point is mean ± SE of three replicate boxes (b–e) or 12 plants (f, g). $*P < 0.05$, $**P < 0.01$, $***P < 0.001$ according to Student's *t*-tests or factorial ANOVA followed by Bonferroni post-tests.

In experiments where the seedlings were grown under long days (16 h white light/8 h in the dark), the 84461-2 mutant showed a reduced cotyledon area (11 days, Figure 1f). Flowering time was accelerated in 84461-2 mutant plants grown under long days and normal under short days (8 h white light/16 h in the dark) (Figure 1g).

The 84461-2 mutant phenotype is caused by overexpression of ROC1

A single T-DNA insertion was found in the 84461-2 mutant by using thermal asymmetric interlaced polymerase chain reaction (TAIL-PCR) (Liu *et al.*, 1995). This T-DNA was inserted in a *gypsy*-like retrotransposon (*At3g60935*), a locus unlikely to be responsible for the phenotype, suggesting that the phenotype could be due to the cDNA fragment present in the T-DNA. The 3:1 mutant/WT ratio observed in the blue-light-grown F_2 population of the cross between the 84461-2 mutant and the WT (Col-2) indicated a dominant mutation responsible for the 84461-2 phenotype. In the F_2 generation, blue light hyposensitivity co-segregated with the resistance to Basta conferred by the T-DNA, and with PCR products obtained by using specific primers adjacent to the cDNA (PCR positive/herbicide resistant, 65 plants; PCR negative/herbicide sensitive, 21 plants; other combinations, 0 plants; chi-square test, $P < 5 \times 10^{-20}$). Sequencing the latter PCR product of approximately 1 kb revealed the presence of the *At4g38740* gene downstream of the 35S promoter in the T-DNA. This gene encodes a cytoplasmic single-domain cyclophilin named ROC1/AtCYP18-3 (Romano *et al.*, 2004). The 84461-2 mutant showed increased expression levels of *ROC1* (Figure 2a).

To test whether the observed 84461-2 mutant phenotypes result from overexpression of *ROC1*, we transformed Col-2 plants with *ROC1* cDNA under the control of the 35S promoter. Independent transgenic lines overexpressing *ROC1* showed long hypocotyls under blue light (Figure 2b,c). Recapitulation of the 84461-2 mutant phenotype indicates that it is caused by increased expression of *ROC1*, which is in agreement with the dominant phenotype observed in the 84461-2 mutant, hereafter named *roc1-1D*.

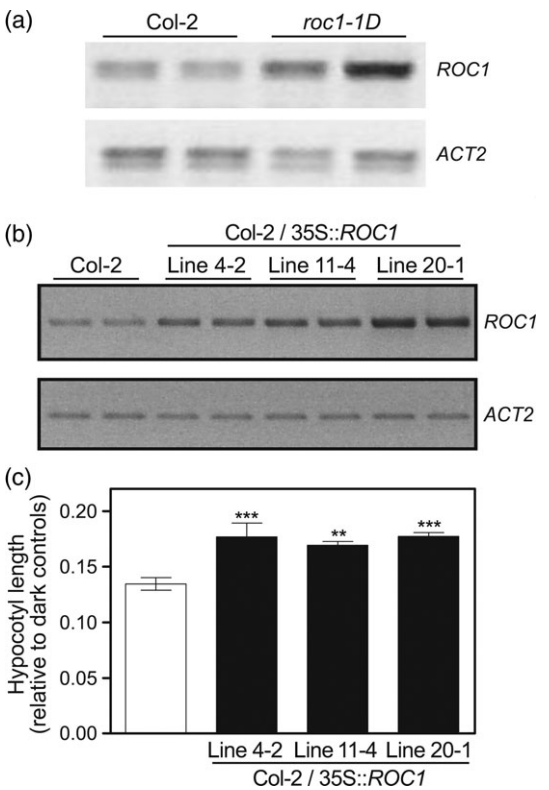

Figure 2. Increased expression of the *ROC1* gene accounts for the 84461-2 mutant phenotype.
(a) *ROC1* expression in the rosette leaves of two independent wild type (WT) and 84461-2 mutant plants (*roc1-1D*). *ACTIN 2* (*ACT2*) was used as a loading control.
(b) *ROC1* expression in three independent transgenic lines (two different seedlings per line) compared to the WT Col-2.
(c) Overexpression of *ROC1* recapitulates the 84461-2 mutant phenotype. Hypocotyl length in seedlings grown for 3 days under continuous blue light (7 μmol m^{-2} per sec). The three independent transgenic lines described in (b) are included. Data are means ± SE of three replicate boxes. $^{**}P < 0.01$, $^{***}P < 0.001$ according to one-way ANOVA followed by Bonferroni post-tests.

Impaired de-etiolation in partial loss-of-function *roc1* mutants

To investigate whether the phenotype of overexpressors of *ROC1* reflects the actual function of the gene, we examined two independent lines bearing a T-DNA insertion in the promoter of the *ROC1* gene [SALK_121820 (*roc1-2*) and SALK_050945 (*roc1-3*)]. Both mutants retained *ROC1* expression, albeit at reduced levels (Figure 3a). Both, *roc1-2* and *roc1-3* showed hyposensitivity of cotyledon unfolding and hypocotyl growth inhibition to blue, far-red and red light (Figure 3b,c). The effects were stronger at higher fluence rates, and to highlight this feature we plotted the ratio of hypocotyl length between *roc1* mutants and Col-0 WT for each irradiance level (Figure 3b, bottom boxes). Both mutants showed increased anthocyanin accumulation under continuous far-red light (Figure 3d). The *roc1-2* mutation, but not the *roc1-3* mutation, enhanced anthocyanin accumulation under continuous blue light and blocking of greening by far-red light (Figure 3d,e). Cotyledon area under white light was increased in *roc1* mutants compared with the WT (Figure 3f). Both *roc1* mutant alleles showed slightly accelerated flowering under long days and normal flowering under short days (Figure 3g). In summary, hypocotyl growth and cotyledon unfolding responses under far-red and blue light were reduced, and flowering under long days was accelerated both by the high levels of *ROC1* in the *roc1-1D* mutant and the reduced levels of *ROC1* in *roc1*. The other phenotypes were opposite in gain- and loss-of-function mutants: cotyledon unfolding under red light was enhanced in *roc1-1D* and reduced in loss-of-function *roc1*;

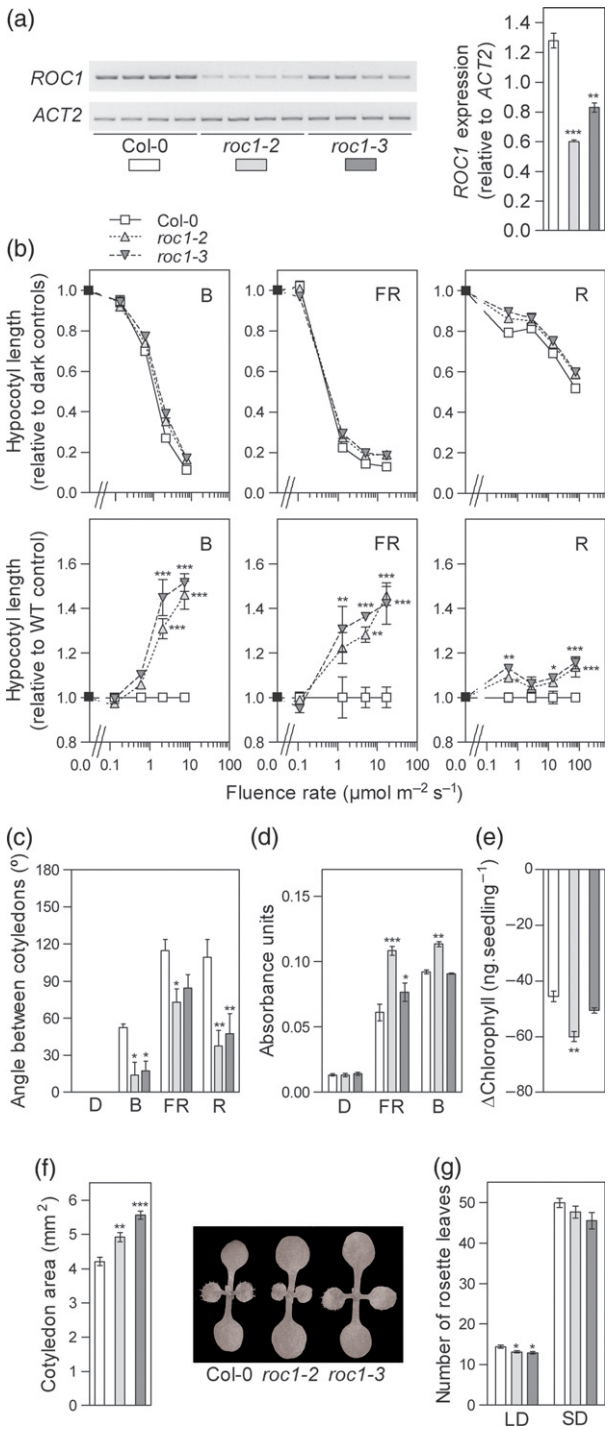

Figure 3. Impaired photomorphogenesis in partial loss-of-function *roc1* mutants.

(a) Expression levels of *ROC1* in the rosette leaves of the wild type (WT; Col-0) and two *roc1* T-DNA insertional mutants (two independent plants per genotype, two samples per plant). (b) Fluence-rate response of hypocotyl length under continuous blue (B), far-red (FR) or red (R) light. Bottom boxes display the *roc1*/WT ratio (data from top boxes). (c) Cotyledon unfolding under B (0.18 μmol m^{-2} per sec), FR (0.5 μmol m^{-2} per sec) or R light (1.8 μmol m^{-2} per sec) or darkness (D).

(d) Anthocyanin levels under continuous FR light (15 μmol m^{-2} per sec), B light (15 μmol m^{-2} per sec) or D. (e) Blocking of greening by continuous FR light (3 days, 7 μmol m^{-2} per sec) compared with darkness before transfer to fluorescent white light (1 day, 30 μmol m^{-2} per sec) (difference in chlorophyll content between darkness and FR light). (f) Cotyledon area in seedlings grown under long days (16 h of fluorescent white light, 8 h of darkness). (g) Flowering time (number of rosette leaves at bolting) under short days (SD, 8 h of fluorescent white light, 16 h of darkness) or long days (LD, 16 h of fluorescent white light, 8 h of darkness).

Seedlings were 3 (b–e) or 11 (f) days old. Each datum point is mean ± SE of three replicate boxes (b–e) or 12 plants (f, g). $*P < 0.05$, $**P < 0.01$, $***P < 0.001$ according to factorial ANOVA followed by Bonferroni post-tests.

anthocyanin accumulation, blocking of greening and cotyledon area were reduced in the *roc1-1D* mutant and enhanced in loss-of-function *roc1*.

Light promotes the expression of ROC1

Since *roc1* mutants affect seedling photomorphogenesis we investigated the response of *ROC1* expression to light. Compared with darkness, blue, red and far-red light promoted *ROC1* expression (Figure S1 in Supporting Information), confirming previous observations (Chou and Gasser, 1997; Tepperman *et al.*, 2004, 2006; Zimmermann *et al.*, 2004; Sellaro *et al.*, 2009). These effects are mediated by cry1 (Sellaro *et al.*, 2009), phyA and phyB (Tepperman *et al.*, 2004, 2006).

The *roc1* phenotype requires *phyA, phyB* and *cry1* under selective wavebands

We produced double mutants of *roc1-2* with *phyA*, *phyB* and *cry1* and the triple mutant with *phyA* and *cry1*. The *phyA, phyB* and *phyA cry1* backgrounds, respectively, abolished the *roc1* phenotype under far-red light (Figure 4a), red light (Figure 4b) and blue light (Figure 4c). We therefore conclude that the *roc1* phenotype requires phyA under far-red light, phyB under red light and either phyA or cry1 under blue light. The *phyA cry1 roc1* triple mutant was not significantly different from the *phyA cry1* double mutant, indicating that the contribution of cry2 to the *roc1* phenotype under blue light is negligible.

ROC1 affects sensitivity to brassinosteroids

The *diageotropica* (*dgt*) mutant of tomato is affected in the *LeCYP1* cyclophilin gene (Oh *et al.*, 2006) and shows altered sensitivity to auxin (Daniel *et al.*, 1989; Muday *et al.*, 1995), cytokinin (Coenen and Lomax, 1998) and brassinosteroid (Park, 1998). Taking into account the sequence similarity between *ROC1*/*AtCYP18-3* and *LeCYP1* (Oh *et al.*, 2006) we decided to investigate the responses to exogenous application of the synthetic auxin picloram (Hansen and Grossmann, 2000), the natural cytokinin *t*-zeatin and the natural brassinosteroid 24-epiBL in *roc1* and *roc1-1D* mutants. In dark-grown seedlings, exogenously applied auxin reduces hypocotyl growth; whereas in light-grown seedlings, auxin promotes hypocotyl elongation at low doses and inhibits

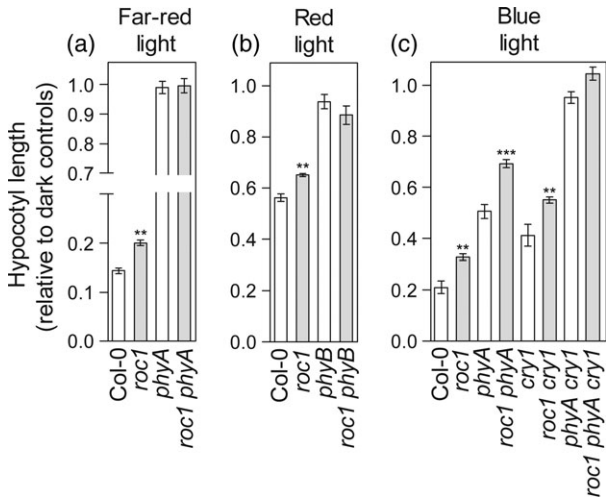

Figure 4. *phyA, phyB* and *cry1* mutations abolish the *roc1* phenotype
Seedlings were grown under continuous far-red light (6 μmol m^{-2} per sec) (a), red light (30 μmol m^{-2} per sec) (b), blue light (4 μmol m^{-2} per sec) (c), or darkness. Data are means ± SE of three replicate boxes. $^{**}P < 0.01$, $^{***}P < 0.001$ between the *ROC1* (white column) and *roc1-2* (grey column) alleles for each photoreceptor genetic background according to factorial ANOVA followed by Bonferroni post-tests.

hypocotyl elongation at high doses (Savaldi-Goldstein *et al.*, 2008). Cytokinin inhibits hypocotyl elongation in both dark- and light-grown seedlings (Vandenbussche *et al.*, 2007). The *roc1* and *roc1-1D* mutants showed WT responses to auxin or cytokinin under blue light (note parallel curves) and in the dark (Figure S2). Brassinosteroids can promote hypocotyl elongation under light and dark conditions, but concentrations above 0.1 μM can inhibit growth in the dark (Neff *et al.*, 1999; Vandenbussche *et al.*, 2007). The *roc1* and *roc1-1D* mutants showed WT responses to 24-epiBL in the dark (Figure 5a). Under blue light, 1 μM 24-epiBL reduced hypocotyl growth in *roc1* and *roc1-1D* mutants but not in the WT, suggesting a higher sensitivity to exogenous brassinosteroids (Figure 5b). To explore this possibility we investigated in further detail the response to low doses of brassinosteroids. In Figure 5(c) hypocotyl length in the absence of brassinosteroids is subtracted to focus on the response to 24-epiBL. Both *roc1* and *roc1-1D* mutants showed an enhanced response to 24-epiBL. We also tested the sensitivity to brassinazole, an inhibitor of brassinosteroid biosynthesis (Asami *et al.*, 2000). The *roc1* and *roc1-1D* mutants showed WT responses to brassinazole in the dark,

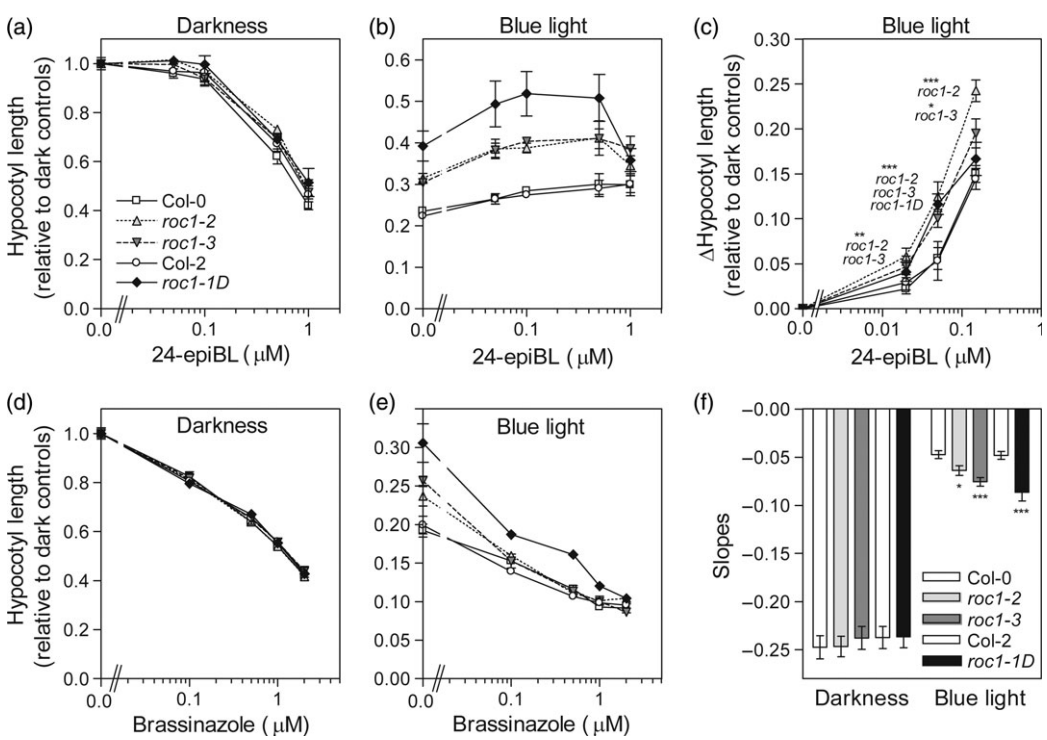

Figure 5. The *roc1-1D, roc1-2* and *roc1-3* mutants are hypersensitive to exogenous natural brassinosteroid (24-epiBL) and brassinazole under blue light.
(a) Hypocotyl-length response to 24-epiBL in dark-grown seedlings. (b) Hypocotyl-length response to 24-epiBL under continuous blue light (4 μmol m^{-2} per sec). (c) Detail of the hypocotyl-length response to 24-epiBL under continuous blue light at low doses of 24-epiBL. Hypocotyl length of the controls without 24-epiBL for each genotype was subtracted to highlight the differences in the slope of response to 24-epiBL. (d) Hypocotyl-length response to brassinazole in dark-grown seedlings. (e) Hypocotyl-length response to brassinazole under continuous blue light (4 μmol m^{-2} per sec). (f) Slope of linear regression lines from the brassinazole response curves (d, e).
Data are means ± SE of four replicate boxes (a, b, d, e). In (c), the difference in hypocotyl length between seedlings at a given dose and the control without 24-epiBL was calculated for each genotype in three independent experiments (four replicate boxes per experiment) and these differences were used for statistics. $^{*}P < 0.05$, $^{**}P < 0.01$, $^{***}P < 0.001$ between the mutant and the corresponding wild type according to factorial ANOVA and Bonferroni post-tests.

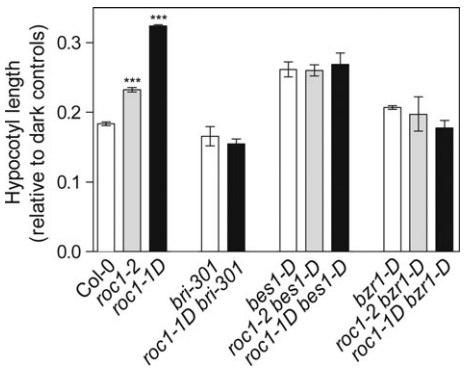

Figure 6. Brassinosteroid signalling mutants abolish the *roc1* phenotype.
Seedlings were grown under continuous blue light (4 μmol m^{-2} per sec) or darkness. Data are means ± SE of three replicate boxes. ***$P < 0.001$ between *roc1-2* or *roc1-1D* and the wild type (Col-0) according to one-way ANOVA followed by Bonferroni post-tests.

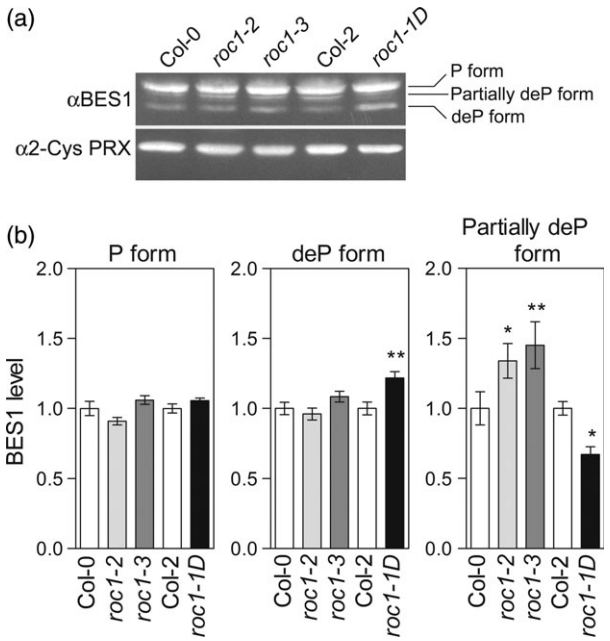

Figure 7. Altered pattern of BES1 phosphorylation in the *roc1-1D*, *roc1-2* and *roc1-3* mutants.
One-day-old dark-grown seedlings were transferred to blue light (4 μmol m^{-2} per sec) for 3 days.
(a) Representative autoradiograph revealed by using anti-BES1 antibody and anti-2-Cys-Prx as a loading control. P = phosphorylated form, deP = dephosphorylated form.
(b) Quantification of the abundance of the phosphorylated, dephosphorylated and partially dephosphorylated forms of BES1. Data are expressed relative to the wild-type controls (Col-0 for *roc1-2* and *roc1-3* alleles and Col-2 for *roc1-1D*). Data are means ± SE of three blots with independent biological samples. **$P < 0.01$ according to one-way ANOVA followed by Bonferroni post-tests.

and a steeper response to brassinazole under blue light (Figure 5d,e), indicating that the *roc1* and *roc1-1D* phenotypes require brassinosteroids. Figure 5(f) shows that the slope of the response to brassinazole is reduced by blue light in a *ROC1*-dependent manner.

The *roc1* and *roc1-1D* mutant phenotypes require brassinosteroid signalling

The addition of brassinazole alleviated the *roc1* and *roc1-1D* mutant phenotypes (Figure 5e), suggesting that they require brassinosteroid signalling. To test this possibility we produced double mutants between *roc1* or *roc1-1D* and brassinosteroid-signalling mutants. We used *bes1-D* (Yin *et al.*, 2002) and *bzr1-D* (He *et al.*, 2002; Wang *et al.*, 2002b), gain-of-function mutants of two homologous transcription factors acting positively in brassinosteroid signalling, and the weak loss-of-function mutant of brassinosteroid receptor *bri1-301* (Xu *et al.*, 2008). The *bri1 roc1* double mutant could not be obtained due to the very close location of both genes on chromosome IV. The *bes1-D* and *bzr1-D* mutations abolished the *roc1* and *roc1-1D* mutant phenotypes for hypocotyl growth under blue light (Figure 6). The *bri1* mutation also abolished the *roc1-1D* mutant phenotype (Figure 6).

Altered patterns of phosphorylation of BES1 in the *roc1-1D* and *roc1* mutants

Given that enhanced BES1 activity abolished the *roc1-2* and *roc1-1D* mutant phenotypes we decided to investigate the abundance and phosphorylation status of BES1 (Li, 2010) in our mutants. Protein blots using an antibody able to detect both forms of BES1 revealed no differences for the phosphorylated (inactive) form of BES1 in the different genotypes. Interestingly, we detected higher levels of the dephosphorylated (active) BES1 form in *roc1-1D* (Figure 7). The *roc1-2* and *roc1-3* alleles showed increased abundance of a partially dephosphorylated form of BES1, whose abundance was decreased in *roc1-1D* (Figure 7).

Since cyclophilins possess peptidyl–prolyl *cis–trans* isomerase activity, and in both *bes1-D* and *bzr1-D* the mutations affect a Pro residue important for the stability and function of the proteins (Yin *et al.*, 2002; Tang *et al.*, 2011; see Discussion), we decided to assess whether ROC1 is able to interact with BES1 or with its immediate upstream regulator, the GSK3 kinase BIN2.Yeast two-hybrid assays using a WT and the mutant form of BES1 (BES1-D, Pro-233 to Leu) and WT BIN2 yielded negative results (Figure S3).

Expression of genes directly targeted by BES1

We reasoned that if the effects of ROC1 on BES1 phosphorylation are physiologically important they should be reflected in the expression of genes directly targeted by BES1. To investigate this issue, we selected 11 genes that are direct targets of BES1 (Yu *et al.*, 2011) and show expression affected in *bes1-D* compared with the WT (Yu *et al.*, 2011), by brassinosteroids (Yu *et al.*, 2011) and by light compared with darkness (Zimmermann *et al.*, 2004) in previous studies. At least three biological replicates of *roc1-1D*, *roc1-2*, *roc1-3*,

Col-0 and Col-2 were grown under blue light and harvested for RNA extraction and analysis of gene expression by real-time PCR. Of the 11 genes, nine showed expression levels that correlated with the levels of the partially dephosphorylated form of BES1 (i.e. the form significantly affected in the three mutants compared with their WT) (Figure 8). All these nine genes showed a direction of response consistent with increased BES1 activity. In effect, eight of these genes (*At1g69160*, *At4g31820*, *At1g72180*, *At1g76240*, *At4g17460* and the brassinosteroid synthesis genes *At5g05690*, *At3g50660*, *At4g36380*) show expression reduced in *bes1-D* compared with the WT and by the application of brassinosteroids (Yu *et al.*, 2011) and their expression levels were negatively related to the partially dephosphorylated form of BES1 (Figure 8). The remaining gene (*At1g21910*) shows expression promoted in *bes1-D* compared with the WT and by the application of brassinosteroids (Yu *et al.*, 2011), and its level of expression was positively related to the partially dephosphorylated form of BES1 (Figure 8). Of the two genes without significant correlation with partially dephosphorylated BES1, *At1g29395* expression was significantly reduced in *roc1-1D* compared with the WT (Col-2, 1.00 ± 0.11; *roc1-1D*, 0.40 ± 0.03) and unaffected by *roc1-2* or *roc1-3* mutations. The effects were largely light specific because in dark-grown seedlings none of these genes showed consistent effects of both *roc1* loss-of-function mutations and the *At1g69160* gene showed reduced expression in *roc1-D* compared with its WT (Table S1), whilst under blue light *roc1-1D* promoted the expression of this gene (Figure 8).

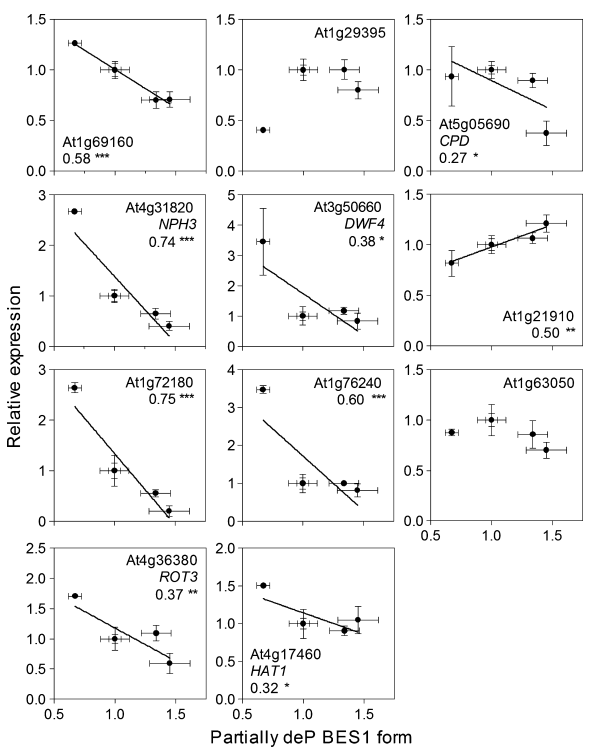

Figure 8. Expression of genes directly targeted by BES1 in seedlings of *roc1-1D*, *roc1-2* and *roc1-3* grown under blue light.
Eleven genes were selected *a priori* among direct targets of BES1 by their consistent expression responses to the *bes1-D* mutation and brassinosteroids and their response to blue light. Expression levels relative to the corresponding wild type are plotted against the abundance of the partially dephosphorylated form of BES1 (data from Figure 7b), i.e. the first point on the abscissa corresponds to *roc1-1D*, the second two points (overlapped) correspond to Col-0 and Col-2 and the last two points to *roc1-2* and *roc1-3*. R^2 values are indicated for significant correlations: $^*P < 0.05$; $^{**}P < 0.01$; $^{***}P < 0.001$; $^{****}P < 0.0001$. Each datum point is mean and SE of at least three biological replicates (i.e. analysis of correlation involves at least 15 biological replicates).

DISCUSSION

By screening for mutants under blue plus far-red light we have identified the dominant *roc1-1D* mutant with long hypocotyls under blue and under far-red light (Figure 1). The *roc1-1D* mutant shows elevated expression of the *ROC1*/*AtCYP18-3* cyclophilin gene and transgenic overexpression of *ROC1* in the WT background recapitulated the *roc1-1D* phenotype (Figure 2). Partial loss-of-function *roc1* alleles showed long hypocotyls under blue, far-red and red light (Figure 3). Other seedling phenotypes (cotyledon unfolding under red light, anthocyanin accumulation, blocking of greening, cotyledon expansion) were opposite in gain- and loss-of function mutants (Figures 1 and 3). Cyclophilins are present in all organisms examined including bacteria, fungi, animals and plants, and possess peptidyl–prolyl *cis–trans* isomerase activity, catalysing the rotation of X-Pro peptide bonds from *cis* to *trans* conformation, a rate-limiting step in protein folding (Romano *et al.*, 2004). Over 90% of proteins contain *trans* prolyl imide bonds (Romano *et al.*, 2004). Arabidopsis ROC1 is a cytosolic single-domain cyclophilin that had been reported to assist in the folding of the *Pseudomonas syringae* AvrRpt2 effector protein upon infection of the plant host (Coaker *et al.*, 2005, 2006). Therefore, ROC1 is involved in functions beyond light signalling.

The *diageotropica* (*dgt*) mutant of tomato shows altered sensitivity to auxin (Daniel *et al.*, 1989; Muday *et al.*, 1995), cytokinin (Coenen and Lomax, 1998) and brassinosteroids (Park, 1998). *dgt* is affected in the *LeCYP1* cyclophilin gene (Oh *et al.*, 2006), bearing significant sequence similarity to the Arabidopsis *ROC1*/*AtCYP18-3*. The *roc1-1D* and *roc1-2*, *roc1-3* alleles showed normal responses to exogenous auxin and cytokinin (Figure S2). However, these mutants showed high sensitivity to the brassinosteroid 24-epiBL and to the brassinosteroid synthesis inhibitor brassinazole (Figure 5). The latter phenotypes were observed under light but not under dark conditions. A partial loss-of-function mutation at the brassinosteroid receptor gene BRI1 (Xu *et al.*, 2008) and gain-of-function mutations at the BRI1 downstream transcription factors BES1 (Yin *et al.*, 2002) or BZR1 (He *et al.*, 2002; Wang *et al.*, 2002b) were abolished the *roc1-1D* and/or *roc1-2* phenotypes (Figure 6). These results indicate that a fully functional BRI1 is necessary for ROC1 to have an effect, and

that this effect can be by-passed by the overactive transcription factors acting downstream in the signalling pathway.

Brassinosteroid and light signalling converge to control several aspects of plant growth and development and mutually affect their activities. This convergence is also reflected in the numerous genes that are targets of both signalling pathways (Goda *et al.*, 2002; Luo *et al.*, 2010; Sun *et al.*, 2010; Yu *et al.*, 2011). Brassinosteroids are required to maintain the repression of photomorphogenesis in the dark (Li *et al.*, 1996). Upon exposure to light, brassinosteroids fine-tune light responses by differentially modulating the action of different photoreceptors (Luccioni *et al.*, 2002).

The *BAS1* and *SOB7* genes encode cytochrome P450 proteins (CYP734A1 and CYP72C1, respectively) that act redundantly to reduce, through hydroxylation, the levels of active brassinosteroids such as brassinolide and castasterone (Neff *et al.*, 1999; Turk *et al.*, 2003, 2005). Since these genes affect active brassinosteroid levels and brassinosteroid signalling modulates light signalling as described above, *bas1* and *sob7* mutants have clear photomorphogenic phenotypes (Neff *et al.*, 1999; Turk *et al.*, 2003, 2005). Our knowledge of the putative points of reciprocal control, i.e. the occurrence of targets of light signalling within the core brassinosteroid signalling pathways, is much more fragmentary. One example is provided by the CYP734A1 (BAS1) protein, whose accumulation is increased by far-red light, suggesting a far-red light-induced reduction of active brassinosteroid levels (Turk *et al.*, 2003). This control would not be present under red or blue light (Turk *et al.*, 2003), which is consistent with the lack of reductions in brassinosteroid levels under white light (Neff *et al.*, 1999; Bancos *et al.*, 2006; Symons and Reid, 2008; Symons *et al.*, 2008). Another example is provided by *MSBP1*, whose expression is promoted by light via the transcription factors HY5 and HYH (Shi *et al.*, 2011). MSBP1 binds brassinosteroids, reducing their activity (Yang *et al.*, 2005). One of the distinctive features of *ROC1* overexpression or loss-of-function growth phenotypes is that they are strictly dependent on light perceived by cry1, phyA or phyB (Figure 4) (in contrast to *BAS1* or MSBP1) and strictly dependent on brassinosteroid signalling (Figure 6).

Light is likely to reduce the sensitivity to brassinosteroids under the conditions where it does not reduce active brassinosteroid levels (Neff *et al.*, 1999; Turk *et al.*, 2003; Vandenbussche *et al.*, 2007). The *roc1-1D*, *roc1-2* and *roc1-3* mutants have increased sensitivity to exogenous 24-epiBL and to the brassinosteroid synthesis inhibitor brassinazole under blue light but not in the dark (Figure 5). It is difficult to account for the *roc1* phenotypes on the basis of altered levels of endogenous brassinosteroids. One of the arguments against this idea is that the gain-of-function *bes1-D* and *bzr1-D* mutants fully abolished the *roc1* phenotypes (Figure 4). Since *bes1-D* and *bzr1-D* are hypersensitive to brassinosteroids (He *et al.*, 2002; Yin *et al.*, 2002), if *roc1* mutants had higher brassinosteroid levels their phenotype should not be reduced by the *bes1-D* and *bzr1-D* mutations under blue light, where brassinosteroids are not saturating (see Figure 5). This analysis suggests that ROC1 could affect the response to brassinosteroids at or downstream of BES1 and/or BZR1. In accordance with this prediction we observed BES1 phosphorylation phenotypes in the *roc1* and *roc1-1D* mutants (Figure 7).

The level of a partially dephosphorylated form of BES1 was increased in the *roc1* loss-of-function mutants and decreased in the *roc1-D* mutant, i.e. the abundance of the partially dephosphorylated form of BES1 was inversely related to *ROC1* expression levels (Figure 7). BES1/BZR1 have several possible GSK3 phosphorylation sites, including a central region with a stretch of Pro-associated Ser/Thr (Peng *et al.*, 2010) and the N-terminal DNA-binding domain (Vert and Chory, 2006). Therefore, the occurrence of intermediate phosphorylation stages is not surprising and can be observed in published protein blots (Tang *et al.*, 2011). It is notable that the PEST region of BES1 and BZR1 contains a proline residue at positions 233 and 234, respectively, that is crucial for activity (He *et al.*, 2002; Yin *et al.*, 2002). In fact, these prolines and the residues surrounding them form the interaction surface with B′ subunits of the PP2A phosphatase that dephosphorylates and activates BZR1 upon brassinosteroid perception (Tang *et al.*, 2011). Peptidyl–prolyl *cis–trans* isomerases can participate in complexes that regulate phosphorylation. One example is Pin1, which controls phosphorylation and consequently turnover rates of the c-Myc proto-oncoprotein (Arnold *et al.*, 2009). Pin1 recognises c-Myc phosphorylated by the GSK3β kinase and causes c-Myc *cis* to *trans* isomerisation and its subsequent dephosphorylation at a different site by the PP2A-B56α phosphatase. ROC1 and BES1 showed no physical interaction in double-hybrid assays in yeast (Figure S3), indicating that either this effect is indirect or that physical interaction between ROC1 and BES1 requires other factors present *in planta*. Actually, some peptidyl–prolyl *cis–trans* isomerases only recognise phosphorylated substrates (Arnold *et al.*, 2009; Wang *et al.*, 2010).

Dephosphorylation of BES1 and BZR1 increases their activity (He *et al.*, 2002; Yin *et al.*, 2002; Vert and Chory, 2006; Clouse, 2011). The expression of several BES1 direct target genes was correlated with the level of the partially dephosphorylated form of BES1 across the different genotypes in the same direction as they respond to increased BES1 activity and brassinosteroid treatments (Figure 8). The analysis of a phenotype close to the primary action of BES1 (i.e. the expression of its direct target genes) showed opposite effects for the *roc1-1D* mutant overexpressing *ROC1* and the partial loss-of-function *roc1* alleles. Opposite effects were also observed for cotyledon unfolding under red light, anthocyanin accumulation, blocking of greening and cotyledon expansion (Figures 1 and 3). However, inhibition of

hypocotyl growth and cotyledon unfolding under far-red light and blue light and flowering in long days were affected by *roc1-1D* and the partial loss-of-function *roc1* alleles in the same direction (Figures 1 and 3). The latter effects of *roc1-1D* do not necessarily reflect the real role of ROC1 in development. Rather, they could be downstream consequences of the changes in abundance of the fully dephosphorylated form of BES1, in the expression of At1g29395 under blue light and in the expression of At1g69160 in the dark, which are observed in *roc1-1D* but not in the *roc1* partial loss-of-function alleles.

We propose a model where light activation of phytochromes and cryptochromes enhances ROC1 activity, at least in part by increasing the expression of *ROC1* (Chou and Gasser, 1997; Tepperman *et al.*, 2004, 2006; Zimmermann *et al.*, 2004; Sellaro *et al.*, 2009) (Figure S1). In turn, ROC1 decreases the abundance of the partially dephosphorylated form of BES1 (Figure 7) and reduces BES1 activity (Figure 8), reducing the sensitivity to brassinosteroids (Figure 5) and fine-tuning de-etiolation (Figure 3).

EXPERIMENTAL PROCEDURES

Mutant screening

For the mutant screening we used seeds of *A. thaliana* ecotype Columbia (Col-2) transformed with a T-DNA library based on the 35SpBARN vector produced by LeClere and Bartel (2001). The seeds were sown in plastic boxes containing 0.8% (w/v) agar covered with a filter paper, incubated for 7 days at 4°C to reduce dormancy levels. Germination was induced by 1 h of white light followed by 23 h in the dark and then transferred to continuous blue plus far-red light at 22°C for 3 days before screening for seedlings with long hypocotyls. Blue plus far-red light was provided by incandescent lamps (CLAS A CL 40W; Osram, Beccar, Argentina) and fluorescent lamps (TLD 36W/54; Philips, Jakarta, Indonesia) in combination with a 2-mm-thick blue acrylic filter (Paolini 2031; La Casa del Acetato, Buenos Aires, Argentina).

Physiological experiments

The *roc1-2* (SALK_121820, T-DNA inserted between 310 and 554 bp upstream of the start codon), *roc1-3* (SALK_050945, T-DNA inserted between 249 and 554 bp upstream of the start codon), *phyA* (SALK_014575), *phyB* (SALK_069700) and *cry1* (SALK_069292) mutants in the Col-0 background were provided by the Arabidopsis Biological Resource Center (ABRC; Ohio State University, Columbus, OH, USA). The primers used to genotype these mutants are given in Table S2. The *bzr1-D* (Wang *et al.*, 2002b) and *bri1-301* (Li and Nam, 2002) in the Columbia background, and the *bes1-D* mutant in the En-2 background (Yin *et al.*, 2002) introgressed for seven rounds into the Columbia (Col-0) background were included in some experiments. Double and triple mutants bearing homozygous *bzr1-D*, *bri1-301* and *bes1-D* alleles were detected by the characteristic adult phenotype of these mutant plants showing no segregation in subsequent generations. The seeds (16–20 for morphological and 60 for chlorophyll and anthocyanin experiments) were sown in clear plastic boxes [40 mm × 33 mm × 15 mm (height)] containing 4 ml of 0.8% (w/v) agar. However, for the experiments involving exogenous hormones, the seeds were sown on two Whatman No. 5 filter papers soaked in water solutions containing picloram (Tordon 24K, Dow AgroSciences, Buenos Aires, Argentina), *t*-zeatin (Sigma Chemical Co., St Louis, MO, USA), 24-epiBL (Sigma Chemical Co.) or brassinazole (kindly provided by Tadao Asami, Riken, Japan). These products were dissolved in water (picloram), ethanol (24-epiBL) or DMSO (brassinazole, *t*-zeatin). Controls without hormone treatments included the solvent [8×10^{-3}% (v/v) ethanol or 7×10^{-5}% DMSO). The boxes were incubated in the dark at 4°C for 3–7 days, given 1 h of red light to promote seed germination and incubated in the darkness (22°C) for 23 h.

One-day-old seedlings were transferred to the light treatments (22°C) for 3 days before measurements of hypocotyl length (to the nearest 0.5 mm with a ruler) and angle between the cotyledons (with a protractor) in the 12 tallest seedlings per box. Red and far-red light sources were as described (Casal and Mazzella, 1998). Blue light was provided by fluorescent lamps in combination with a 2-mm-thick blue acrylic filter. Seedling data were averaged per box (one replicate) and used for statistics. White, blue and red light irradiance were measured with a Li-COR LI-188B sensor (Lincoln, NB, USA). Far-red light was measured with a Skye SKR 110 sensor (Skye Instruments Ltd, Llandrindod Wells, Powys, UK) and the values corrected because the spectral range of the far-red light source is wider than the range of sensitivity of the sensor.

For anthocyanin experiments, 1-day-old seedlings were exposed for 3 days to continuous far-red or blue light and subsequently extracted with 1 ml of 1% (w/v) HCl–methanol. Measurements of A_{530} were corrected for chlorophyll absorption (657 nm) according to Mancinelli *et al.* (1991).

For blocking of greening experiments, 1-day-old seedlings were transferred to continuous long-wavelength far-red light provided by incandescent lamps in combination with a water filter and an RG9 filter (Schott, Maintz, Germany), or kept in the dark. Three days later, the seedlings were transferred to continuous fluorescent white light (30 μmol m^{-2} per sec) for 1 day. Fifty seedlings were harvested in *N*,*N*′-dimethylformamide and incubated in the dark at −20°C for at least 3 days. Absorbance was measured in the extracts at 647 and 664 nm, and chlorophyll levels were calculated according to Moran (1982).

Identification of the genetic alteration in the 84461-2 mutant

Polymerase chain reaction was performed using the primers 35S-F and NOS-R to amplify the cDNA insert (LeClere and Bartel, 2001). The amplified DNA of approximately 1 kb was sequenced directly and the sequence analysed with the BLAST program (http://www.arabidopsis.org/Blast/index.jsp). The RNA was purified from plants of the 84461-2 mutant and of the WT by using RNeasy mini columns (Qiagen, Hilden, Germany), including the on-column DNase I digestion described by the manufacturer. Reverse transcription-PCR was performed with 1 μg of RNA and cDNA synthesis by means of the ImProm-II Reverse Trancriptase (Promega, Madison, WI, USA), oligo-dT primer and gene-specific primers (Table S2). Expression of the actin *ACT2* gene was used as a loading control. The number of PCR cycles was 20, based on preliminary calibration experiments for each gene. The products were resolved by electrophoresis in native 1% agarose gels. The PCR-minus-template controls were routinely included and showed negative results.

Generation of ROC1 transgenic plants

For recapitulation of the *roc1-1D* phenotype we transformed Col-2 plants to overexpress the *ROC1* gene. The construction 35S::*ROC1* was generated by PCR amplification of the full-length *At4g38740* gene from the *roc1-1D* mutant using a forward primer hybridising in the 5′ untranslated region and a reverse primer that hybridised in the NOS terminator of the cDNA insert present in the mutant. The reverse primer allows the amplification of the *ROC1* copy present in the T-DNA, lowering the probability of amplifying other cyclophilins with high sequence identity to *ROC1*. Both primers contain attB sites according to Gateway® technology (Invitrogen, Carlsbad, CA, USA).

The PCR product flanked by attB sites was included with pDONR/Zeo in a recombination reaction mediated by the GATEWAY® BP Clonase® following the manufacturer's instructions. The resulting plasmid was cloned in chemically competent *Escherichia coli* DH-5α cells and insertion was confirmed by colony PCR. Plasmid DNA was prepared using the Wizard Miniprep DNA purification system (Promega) followed by sequencing. The plasmid was then mixed with the plant expression vector pK2GW7 (Karimi *et al.*, 2002) and subjected to a GATEWAY® LR Clonase® reaction. The resultant vector was cloned in DH-5α cells confirmed by colony PCR and consequently electroporated into *Agrobacterium tumefaciens* strain GV3101 (Koncz and Schell, 1986). For plant transformation Col-2 seedlings were potted in a periodically fertilised mix of perlite, vermiculite and sphagnum moss peat (1:1:1). Primary inflorescences were removed and secondary inflorescences were allowed to elongate to about 10–20 cm before plants were transformed following the floral-dip method (Clough and Bent, 1998). T_1 seedlings were selected in half-strength MS medium containing 50 mg L^{-1} kanamycin. Rounds of self-pollination and antibiotic selection allowed T_3 stable transformants that were used for the experiments.

Protein blots

Seedlings were harvested, grinded in Laemmli loading buffer and boiled for 5 min at 8000 ***g***. The extracts were centrifuged, and the supernatants were run on a 10% Laemmli SDS-PAGE and transferred to nitrocellulose. Proteins with an apparent mobility between 30 and 60 kDa were probed with an anti-BES1 purified serum (a generous gift of Yanhai Yin, Iowa State University, Ames, IA, USA) and proteins below 30 kDa were probed with an antiserum raised against rapeseed chloroplast 2-Cys peroxiredoxin (a generous gift from Ricardo Wolosiuk, Fundacion Instituto Leloir, Buenos Aires, Argentina). In both cases, blots were developed with ECLTM (GE Healthcare, Piscataway, NJ, USA) and autoradiographs were scanned for quantification using Adobe® Photoshop® CS4.

Analysis of gene expression by real-time PCR

One-day-old seedlings exposed for 3 days to different light or dark conditions were harvested in liquid nitrogen. An RNeasy Plant Mini Kit (Qiagen) was used for total RNA extraction followed by DNase treatment. Complementary DNA derived from this RNA was synthesised using Invitrogen Super-Script III and an oligo-dT primer, and amplified with FastStart Universal SYBR Green Master (Roche, Mannheim, Germany) using the 7500 Real Time PCR System (Applied Biosystems, Foster City, CA, USA) cycler. The primers are described in Table S2. Annealing and extension (1 min) were at 60°C. The PCR-minus-template controls were routinely included and showed negative results. Each primer pair yielded a single peak in melting curves and a single product was confirmed on agarose gels. Contamination by DNA was ruled out by PCR analysis after DNase treatment. Furthermore, three of the gene primers flanked sequences containing one to three introns and the PCR-amplified products of the real-time reaction of these genes showed only the size corresponding to spliced transcripts in agarose gels.

ACKNOWLEDGEMENTS

This work was supported by grants from the University of Buenos Aires (grants no. G044 to JJC and X473 to SM-G), International Centre for Genetic Engineering and Technology (grant no. CRP/ARG07-02 to JJC) and Agencia Nacional de Promoción Científica y Tecnológica (grant no. PICT 1748 to JJC). We thank Yanhai Yin (Iowa State University) and Ricardo Wolosiuk (Fundacion Instituto Leloir) for their provision of antibodies, Tadao Asami (Riken, Japan) and Arabidopsis Biological Resource Center for their provision of seeds.

SUPPORTING INFORMATION

Additional supporting information may be found in the online version of this article:

Figure S1. Blue, red and far-red light promote *ROC1* expression compared with darkness.

Figure S2. The *roc1-1D*, *roc1-2* and *roc1-3* mutants have normal responses to exogenous auxin and cytokinin.

Figure S3. Yeast two-hybrid assay reveals no physical interaction between ROC1 and different brassinosteroid signalling components.

Table S1. Expression of genes directly targeted by BES1 in dark-grown seedlings of *roc1-1D*, *roc1-2* and *roc1-3*.

Table S2. List of primers.

Please note: As a service to our authors and readers, this journal provides supporting information supplied by the authors. Such materials are peer-reviewed and may be re-organized for online delivery, but are not copy-edited or typeset. Technical support issues arising from supporting information (other than missing files) should be addressed to the authors.

REFERENCES

Ahmad, M. and Cashmore, A.R. (1993) HY4 gene of *A. thaliana* encodes a protein with characteristics of a blue-light photoreceptor. *Nature*, **366**, 162–166.

Arnold, H.K., Zhang, X., Daniel, C.J., Tibbitts, D., Escamilla-Powers, J., Farrell, A., Tokarz, S., Morgan, C. and Sears, R.C. (2009) The Axin1 scaffold protein promotes formation of a degradation complex for c-Myc. *EMBO J.* **28**, 500–512.

Asami, T., Min, Y.K., Nagata, N., Yamagishi, K., Takatsuto, S., Fujioka, S., Murofushi, N., Yamaguchi, I. and Yoshida, S. (2000) Characterization of brassinazole, a triazole-type brassinosteroid biosynthesis inhibitor. *Plant Physiol.* **123**, 93–100.

Bancos, S., Szatmari, A.-M., Castle, J., Kozma-Bognar, L., Shibata, K., Yokota, T., Bishop, G.J., Nagy, F. and Szekeres, M. (2006) Diurnal regulation of the brassinosteroid-biosynthetic CPD gene in Arabidopsis. *Plant Physiol.* **141**, 299–309.

Barnes, S.A., Nishizawa, N.K., Quaggio, R.B., Whitelam, G.C. and Chua, N.-H. (1996) Far-red light blocks greening of Arabidopsis seedlings via a phytochrome A–mediated change in plastid development. *Plant Cell*, **8**, 601–615.

Casal, J.J. and Mazzella, M.A. (1998) Conditional synergism between cryptochrome 1 and phytochrome B is shown by the analysis of phyA, phyB, and hy4 single, double, and triple mutants in Arabidopsis. *Plant Physiol.* **118**, 9–25.

Cashmore, A.R., Jarillo, J.A., Wu, Y.J. and Liu, D. (1999) Cryptochromes: blue light receptors for plants and animals. *Science*, **284**, 760–765.

Chen, M., Chory, J. and Fankhauser, C. (2004) Light signal transduction in higher plants. *Annu. Rev. Genet.* **38**, 87–117.

Chou, I.T. and Gasser, C.S. (1997) Characterization of the cyclophilin gene family of *Arabidopsis thaliana* and phylogenetic analysis of known cyclophilin proteins. *Plant Mol. Biol.* **35**, 873–892.

Clough, S.J. and Bent, A.F. (1998) Floral dip: a simplified method for Agrobacterium-mediated transformation of *Arabidopsis thaliana*. *Plant J.* **16**, 735–743.

Clouse, S.D. (2011) Brassinosteroid signal transduction: from receptor kinase activation to transcriptional networks regulating plant development. *Plant Cell*, **23**, 1219–1230.

Coaker, G., Falick, A. and Staskawicz, B. (2005) Activation of a phytopathogeneic bacterial effector protein by a eukaryotic cyclophilin. *Science*, **308**, 506–508.

Coaker, G., Zhu, G., Ding, Z., Van Doren, S.R. and Staskawicz, B. (2006) Eukaryotic cyclophilin as a molecular switch for effector activation. *Mol. Microbiol.* **61**, 1485–1496.

Coenen, C. and Lomax, T.L. (1998) The DIAGEOTROPICA gene differentially affects auxin and cytokinin responses throughout development in tomato (*Lycopersicon esculentum* Mill.). *Plant Physiol.* **117**, 63–72.

Daniel, S.G., Rayle, D.L. and Cleland, R.E. (1989) Auxin physiology of the tomato mutant diageotropica. *Plant Physiol.* **91**, 804–807.

Duek, P.D. and Fankhauser, C. (2003) HFR1, a putative bHLH transcription factor, mediates both phytochrome A and cryptochrome signaling. *Plant J.* **34**, 827–836.

Goda, H., Shimada, Y., Asami, T., Fujioka, S. and Yoshida, S. (2002) Microarray analysis of brassinosteroid-regulated genes in Arabidopsis. *Plant Physiol.* **130**, 1319–1334.

Guo, H., Mockler, T., Duong, H. and Lin, C. (2001) SUB1, an Arabidopsis Ca^{2+}-binding protein involved in cryptochrome and phytochrome coaction. *Science*, **291**, 487–490.

Hansen, H. and Grossmann, K. (2000) Auxin-induced ethylene triggers abscisic acid biosynthesis and growth inhibition. *Plant Physiol.* **124**, 1437–1448.

He, J.-X., Gendron, J.M., Yang, Y., Li, J. and Wang, Z.Y. (2002) The GSK3-like kinase BIN2 phosphorylates and destabilizes BZR1, a positive regulator of the brassinosteroid signaling pathway in Arabidopsis. *Proc. Natl Acad. Sci. USA*, **99**, 10185–10190.

Hoecker, U., Tepperman, J.M. and Quail, P.H. (1999) SPA1, a WD-repeat protein specific to phytochrome A signal transduction. *Science*, **284**, 496–499.

Hyun, Y. and Lee, I. (2006) KIDARI, encoding a non-DNA binding bHLH protein, represses light signal transduction in *Arabidopsis thaliana*. *Plant Mol. Biol.* **61**, 283–296.

Jiao, Y., Ma, L., Strickland, E. and Deng, X.W. (2005) Conservation and divergence of light-regulated genome expression patterns during seedling development in rice and Arabidopsis. *Plant Cell*, **17**, 3239–3256.

Jiao, Y., Lau, O.S. and Deng, X.W. (2007) Light-regulated transcriptional networks in higher plants. *Nat. Rev. Genet.* **8**, 217–230.

Karimi, M., Inzé, D. and Depicker, A. (2002) GATEWAY vectors for Agrobacterium-mediated plant transformation. *Trends Plant Sci.* **7**, 193–195.

Koncz, C. and Schell, J. (1986) The promoter of TL-DNA gene 5 controls the tissue-specific expression of chimaeric genes carried by a novel Agrobacterium binary vector. *Mol. Gen. Genet.* **204**, 383–396.

LeClere, S. and Bartel, B. (2001) A library of Arabidopsis 35S-cDNA lines for identifying novel mutants. *Plant Mol. Biol.* **46**, 695–703.

Li, J. (2010) Regulation of the nuclear activities of brassinosteroid signaling. *Curr. Opin. Plant Biol.* **13**, 540–547.

Li, J. and Nam, K.H. (2002) Regulation of brassinosteroid signaling by a GSK3/SHAGGY-like kinase. *Science*, **295**, 1299–1301.

Li, J.M., Nagpal, P., Vitart, V., McMorris, T.C. and Chory, J. (1996) A role for brassinosteroids in light-dependent development of Arabidopsis. *Science*, **272**, 398–401.

Lian, H.-L., He, S.-B., Zhang, Y.-C., Zhu, D.-M., Zhang, J.-Y., Jia, K.-P., Sun, S.-X., Li, L. and Yang, H.-Q. (2011) Blue-light-dependent interaction of cryptochrome 1 with SPA1 defines a dynamic signaling mechanism. *Genes Dev.* **25**, 1023–1028.

Lin, C.T., Yang, H.Y., Guo, H.W., Mockler, T., Chen, J. and Cashmore, A.R. (1998) Enhancement of blue-light sensitivity of Arabidopsis seedlings by a blue light receptor cryptochrome 2. *Proc. Natl Acad. Sci. USA*, **95**, 2686–2690.

Liu, Y., Mitsukawa, N., Oosumi, T. and Whittier, R.F. (1995) Efficient isolation and mapping of *Arabidopsis thaliana* T-DNA insert junctions by thermal asymmetric interlaced PCR. *Plant J.* **8**, 457–463.

Liu, B., Zuo, Z., Liu, H., Liu, X. and Lin, C. (2011) Arabidopsis cryptochrome 1 interacts with SPA1 to suppress COP1 activity in response to blue light. *Genes Dev.* **25**, 1029–1034.

Luccioni, L.G., Oliverio, K.A., Yanovsky, M.J., Boccalandro, H.E. and Casal, J.J. (2002) Brassinosteroid mutants uncover fine tuning of phytochrome signaling. *Plant Physiol.* **128**, 173–181.

Luo, X.-M., Lin, W.-H., Zhu, S. *et al.* (2010) Integration of light- and brassinosteroid-signaling pathways by a GATA transcription factor in Arabidopsis. *Dev. Cell*, **19**, 872–883.

Ma, L., Li, J., Qu, L., Hager, J., Chen, Z., Zhao, H. and Deng, X.W. (2001) Light control of Arabidopsis development entails coordinated regulation of genome expression and cellular pathways. *Plant Cell*, **13**, 2589–2607.

Mallappa, C., Yadav, V., Negi, P. and Chattopadhyay, S. (2006) A basic leucine zipper transcription factor, G-box-binding factor 1, regulates blue light-mediated photomorphogenic growth in Arabidopsis. *J. Biol. Chem.* **281**, 22190–22199.

Mancinelli, A.L., Rossi, F. and Moroni, A. (1991) Cryptochrome, phytochrome and anthocyanin production. *Plant Physiol.* **96**, 1079–1085.

Mockler, T.C., Guo, H., Yang, H., Duong, H. and Lin, C. (1999) Antagonistic actions of Arabidopsis cryptochromes and phytochrome B in the regulation of floral induction. *Development*, **126**, 2073–2082.

Moran, R. (1982) Formulae for determination of chlorophyllous pigments extracted with N,N-dimethylformamide. *Plant Physiol.* **69**, 1376–1381.

Muday, G.K., Lomax, T.L. and Rayle, D.L. (1995) Characterization of the growth and auxin physiology of roots of the tomato mutant diageotropica. *Planta*, **195**, 548–553.

Nagatani, A., Reed, J.W. and Chory, J. (1993) Isolation and initial characterization of Arabidopsis mutants that are deficient in phytochrome A. *Plant Physiol.* **102**, 269–277.

Neff, M.M. and Chory, J. (1998) Genetic interactions between phytochrome A, phytochrome B, and cryptochrome 1 during Arabidopsis development. *Plant Physiol.* **118**, 27–35.

Neff, M.M., Nguyen, S.M., Malancharuvil, E.J. *et al.* (1999) BAS1: a gene regulating brassinosteroid levels and light responsiveness in Arabidopsis. *Proc. Natl Acad. Sci. USA*, **96**, 15316–15323.

Oh, K., Ivanchenko, M.G., White, T.J. and Lomax, T.L. (2006) The diageotropica gene of tomato encodes a cyclophilin: a novel player in auxin signaling. *Planta*, **224**, 133–144.

Park, W.J. (1998) Effect of epibrassinolide on hypocotyl growth of the tomato mutant diageotropica. *Planta*, **207**, 120–124.

Parks, B.M. and Quail, P.H. (1993) hy8, a new class of Arabidopsis long hypocotyl mutants deficient in functional phytochrome A. *Plant Cell*, **5**, 39–48.

Peng, P., Zhao, J., Zhu, Y., Asami, T. and Li, J. (2010) A direct docking mechanism for a plant GSK3-like kinase to phosphorylate its substrates. *J. Biol. Chem.* **285**, 24646–24653.

Poppe, C., Sweere, U., Drumm-Herrel, H. and Schafer, E. (1998) The blue light receptor cryptochrome 1 can act independently of phytochrome A and B in *Arabidopsis thaliana*. *Plant J.* **16**, 465–471.

Quail, P.H. (2005) Phytochrome overview. In *Light Sensing in Plants* (Wada, M., Shimazaki, K. and Lino, M., eds). Tokyo: Springer-Verlag, pp. 21–35.

Reed, J.W., Nagpal, P., Poole, D.S., Furuya, M. and Chory, J. (1993) Mutations in the gene for the red/far-red light receptor phytochrome B alter cell elongation and physiological responses throughout Arabidopsis development. *Plant Cell*, **5**, 147–157.

Romano, P.G., Horton, P. and Gray, J.E. (2004) The Arabidopsis cyclophilin gene family. *Plant Physiol.* **134**, 1268–1282.

Savaldi-Goldstein, S., Baiga, T.J., Pojer, F. *et al.* (2008) New auxin analogs with growth-promoting effects in intact plants reveal a chemical strategy to improve hormone delivery. *Proc. Natl Acad. Sci. USA*, **105**, 15190–15195.

Sellaro, R., Hoecker, U., Yanovsky, M., Chory, J. and Casal, J.J. (2009) Synergism of red and blue light in the control of Arabidopsis gene expression and development. *Curr. Biol.* **19**, 1216–1220.

Sellaro, R., Crepy, M., Trupkin, S.A., Karayekov, E., Buchovsky, A.S., Rossi, C. and Casal, J.J. (2010) Cryptochrome as a sensor of the blue/green ratio of natural radiation in Arabidopsis. *Plant Physiol.* **154**, 401–409.

Shi, Q.-M., Yang, X., Song, L. and Xue, H.-W. (2011) Arabidopsis MSBP1 is activated by HY5 and HYH and is involved in photomorphogenesis and brassinosteroid sensitivity regulation. *Mol. Plant*, **4**, 1092–1104.

Sun, Y., Fan, X.-Y., Cao, D.-M. *et al.* (2010) Integration of brassinosteroid signal transduction with the transcription network for plant growth regulation in Arabidopsis. *Dev. Cell*, **19**(5), 765–777.

Symons, G. and Reid, J.B. (2008) Brassinosteroids, de-etiolation and the re-emerging art of plant hormone quantification. *Plant Signal. Behav.* **3**(10), 868–870.

Symons, G.M., Smith, J.J., Nomura, T., Davies, N.W., Yokota, T. and Reid, J.B. (2008) The hormonal regulation of de-etiolation. *Planta*, **227**, 1115–1125.

Tang, W., Yuan, M., Wang, R. *et al.* (2011) PP2A activates brassinosteroid-responsive gene expression and plant growth by dephosphorylating BZR1. *Nat. Cell Biol.* **13**, 124–131.

Tepperman, J.M., Hudson, M.E., Khanna, R., Zhu, T., Chang, S.H., Wang, X. and Quail, P.H. (2004) Expression profiling of phyB mutant demonstrates substantial contribution of other phytochromes to red-light-regulated gene expression during seedling de-etiolation. *Plant J.* **38**, 725–739.

Tepperman, J.M., Hwang, Y.S. and Quail, P.H. (2006) phyA dominates in transduction of red-light signals to rapidly-responding genes at the initiation of Arabidopsis seedling deetiolation. *Plant J.* **48**, 728–742.

Turk, E.M., Fujioka, S., Seto, H., Shimada, Y., Takatsuto, S., Yoshida, S., Denzel, M.A., Torres, Q.I. and Neff, M.M. (2003) CYP72B1 inactivates brassinosteroid hormones: an intersection between photomorphogenesis and plant steroid signal transduction. *Plant Physiol.* **133**, 1643–1653.

Turk, E.M., Fujioka, S., Seto, H. *et al.* (2005) Bas1 and Sob7 act redundantly to modulate Arabidopsis photomorphogenesis via unique brassinosteroid inactivation mechanisms. *Plant J.* **42**, 23–34.

Vandenbussche, F., Habricot, Y., Condiff, A.S., Maldiney, R., Van der Straeten, D. and Ahmad, M. (2007) HY5 is a point of convergence between cryptochrome and cytokinin signalling pathways in *Arabidopsis thaliana*. *Plant J.* **49**, 428–441.

Vert, G. and Chory, J. (2006) Downstream nuclear events in brassinosteroid signalling. *Nature*, **441**, 96–100.

Wang, H., Ma, L., Habashi, J., Li, J., Zhao, H. and Deng, X.W. (2002a) Analysis of far-red light-regulated genome expression profiles of phytochrome A pathway mutants in Arabidopsis. *Plant J.* **32**, 723–733.

Wang, Z.-Y., Nakano, T., Gendron, J. *et al.* (2002b) Nuclear-localized BZR1 mediates brassinosteroid-induced growth and feedback suppression of brassinosteroid biosynthesis. *Dev. Cell*, **2**, 505–513.

Wang, Y., Liu, C., Yang, D., Yu, H. and Liou, Y.C. (2010) Pin1At encoding a peptidyl-prolyl cis/trans isomerase regulates flowering time in Arabidopsis. *Mol. Cell*, **37**, 112–122.

Xu, W., Huang, J., Li, B., Li, J. and Wang, Y. (2008) Is kinase activity essential for biological functions of BRI1? *Cell Res.* **18**, 472–478.

Yadav, V., Mallappa, C., Gangappa, S.N., Bhatia, S. and Chattopadhyay, S. (2005) A basic helix-loop-helix transcription factor in Arabidopsis, MYC2, acts as a repressor of blue light-mediated photomorphogenic growth. *Plant Cell*, **17**, 1953–1966.

Yang, X.H., Xu, Z.H. and Xue, H.W. (2005) Arabidopsis membrane steroid-binding protein 1 is involved in inhibition of cell elongation. *Plant Cell*, **17**, 116–131.

Yi, C. and Deng, X.W. (2005) COP1—from plant photomorphogenesis to mammalian tumorigenesis. *Trends Cell Biol.* **15**, 618–625.

Yin, Y.H., Wang, Z.Y., Mora-Garcia, S., Li, J.M., Yoshida, S., Asami, T. and Chory, J. (2002) BES1 accumulates in the nucleus in response to brassinosteroids to regulate gene expression and promote stem elongation. *Cell*, **109**, 181–191.

Yu, X., Li, L., Zola, J. *et al.* (2011) A brassinosteroid transcriptional network revealed by genome-wide identification of BESI target genes in *Arabidopsis thaliana*. *Plant J.* **65**, 634–646.

Zimmermann, P., Hirsch-Hoffmann, M., Hennig, L. and Gruissem, W. (2004) GENEVESTIGATOR: Arabidopsis microarray database and analysis toolbox. *Plant Physiol.* **136**, 2621–2632.

